Journal of Thermal Analysis and Calorimetry, Vol. 64 (2001) 895–903

THE RELEASE OF STORED ENERGY DURING RECOVERY AND RECRYSTALLIZATION OF COLD ROLLED ULTRA HIGH PURITY IRON

F. Scholz and E. Woldt

Institut für Werkstoffe, Technische Universität Braunschweig, D-38106 Braunschweig, Germany

Abstract

Plastically deformed samples of ultra high purity iron (UHP) doped with 150 ppm of niobium were investigated by differential temperature scanning calorimetry (DTSC) determining the stored energy and the activation enthalpy of recovery and recrystallization. Any oxidation effects were successfully prevented with a newly constructed device for cleaning the specimens by ion-etching and enclosing them hermetically in noble metal capsules without any contact to air. Compared with pure iron the stored energy and the activation enthalpy are increased in the Fe–Nb alloy resulting in a large shift of the recrystallization temperature.

Keywords: preventing of oxidation, recrystallization, stored energy of cold rolled iron

Introduction

Recovery and recrystallization

To some extent all real crystalline solids contain imperfections which distort the strictly regular pattern of the crystal lattice. In the case of the pure metals this paper is concerned with, two types of defects on the atomic scale should be distinguished: point defects, characterised by the local removal/introduction of single atoms and dislocations, line-like defects where the imperfect region extends in one dimension.

Plastic deformation of annealed metallic materials increases the number of lattice defects by several orders of magnitude. Therefore, a certain (but still small) portion of the work expended during deformation is not transformed into heat but retained in the elastic distortion fields surrounding each individual crystal defect. This increase in the Gibbs free energy is known as the stored energy of cold work.

Only on heating the deformed metal to homologous temperatures T/T_{melt} of about 0.5 the density of lattice defects is lowered to the pre-deformed state by two irreversible phenomena called recovery and recrystallization. Recovery means mainly the annealing out of point defects but includes also the annihilation and restructuring of dislocation clusters into energetically more favourable configurations. Recovery is followed by recrystallization, which is a nucleation and growth process. In this case microscopically small strain- and dislocation-free volumes are formed at preferred sites

1418–2874/2001/ $ 5.00

Akadémiai Kiadó, Budapest
Kluwer Academic Publishers, Dordrecht

within the recovered matrix which grow upon further annealing, thereby reducing the dislocation density many times over. The growth of these volumes called grains stops if they impinge on each other and is overall finished if all of the deformed volume has been consumed. As a result of recovery and recrystallization the stored energy is released as heat, and can be observed consequently as exothermal heat flux in a sensitive calorimeter.

Particular difficulties in connection with iron

Both recovery and recrystallization effect several important material properties (e.g. flow stress, texture, volume resistivity etc.). Hence accurate values for the stored energy, representing the driving force for recovery/recrystallization, and the kinetics of the energy release are subject of intensive examinations in this field of research. A number of publications exist dealing with calorimetric measurements of the stored energy in highly deformed face-centred cubic metals (e.g. [1, 2]). On the other hand, investigations of the same kind for body-centred cubic materials are very rare so, in particular, for pure iron, only the unreproduced results of Sato [3] and Taoka *et al.* [4] are available hitherto.

The reason for this remarkable fact may be, first of all, that the stored energy of pure iron is small, and the recrystallization interval extends over a much wider temperature range (~180 K) than e.g. in copper under almost identical circumstances (~20 K) [5]. This results in a much smaller heat flow which can be concealed easily by other reactions, especially by the growth of a scale layer on the specimens owing to the high oxidation capacity of pure iron. In addition, at higher temperatures iron is able to split water vapour [6], and the various iron oxides pass through several phase transformations. Although only a very small volume of the samples participates in all these processes the reaction enthalpies due to their chemical character are much larger than the stored energy signal. For this reason small impurities of oxygen or water vapour in the inert gas used in the calorimeter or even pre-existing oxide layers on the specimens are able to completely ruin the measurement of the stored energy release.

Another point should be mentioned in this context which also makes it necessary to suppress the oxidation of the iron samples: the stored energy peaks observed in this work are so small that they are not clearly visible in the original heat flow measurement (1st run), particularly due to the normal drift of the thermal signal which exists in all DSC investigations. Hence all measurements had to be repeated instantly in order to obtain the baseline (2nd run). The difference of these two runs then eliminates nearly all those parts of the heat flux signal which are due to an imbalance of the calorimeter [7].

However, this procedure requires that the thermal drift is one and the same in both runs. On the other hand, since calorimetric measurements are usually carried out under flowing inert gas ‘unspent’ oxygen is constantly brought over the iron samples so that the oxide layer keeps on growing during both runs. Therefore, the thermal resistance between the specimens and the temperature sensor of the calorimeter in-

creases with time due to the poor thermal conductivity of the iron oxides. This leads to an additional drift and to a change in the slope of the heat flux signal which can not be compensated for by the baseline, but is even amplified in most cases. Consequently the stored energy signal does not appear in the difference between first measured curve and baseline either.

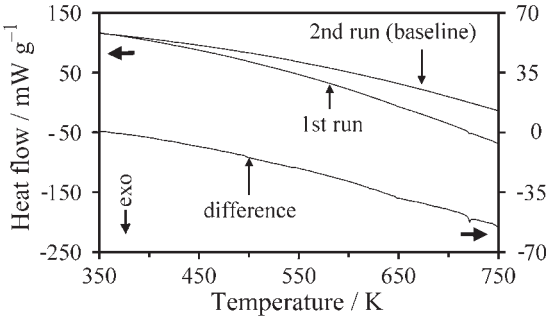

Fig. 1 Consecutive DSC measurements (left scale) of high purity iron (92% rolling deformation, β=20 K min^{-1}) and the heat flow difference of these two runs (right scale). As confirmed by other calorimetric measurements the stored energy peak should occur at about 690 K

This problem is illustrated in Fig. 1 where two successive measurements of the same sample are plotted together with the heat flow difference of these two runs (all exothermic reactions point in the negative y-direction throughout this paper). Neither in the original measurement nor in the subtracted curve the stored energy release can be easily observed since the curvatures of both runs differ too much.

Experimental

Two different materials were used in this study: ultra high purity iron (99.999 mass%) and an UHP Fe-Nb alloy with 150 ppm niobium, which were both prepared at the Microstructure and Processing Department in Saint-Étienne, France [8]. The iron sponges were hot deformed, recrystallized and finally cold-rolled to 80% thickness reduction. Subsequently samples of 6 mm diameter and 2 mm height (~450 mg) well-fitting for the DSC measurements were punched from the rolled strip.

Sample preparation of the UHP Fe

In order to free the surface of the UHP iron samples from already existing oxide layers or other surface contamination mechanical work (e.g. grinding) is not recommended since additional deformations may be introduced. Hence the specimens were ion-etched (sputtered) with argon gas in a commercially available sputter device (Baltec SCD 050) making sure that the temperature did not increased considerably. Of course, hardly any etching takes place at the bottom of the sample supported by the sputter apparatus. Therefore after the first sputtering process the samples were

turned upside down and etched again. This way unhindered access for the etching process to all sides of the specimen was guaranteed. The mass loss due to sputtering was below detection limit (i.e. less than 10 μg).

Attempts were made to avoid the distorting oxidation reactions mentioned above by evacuating the calorimeter. Due to the missing convection of the inert gas within the measuring head the noise level of the heat flow signal increased considerably and became much larger than the stored energy signal. Hence a different approach was adopted. The specimens were hermetically enclosed under 5N-argon gas in well-annealed gold capsules by sealing a lid on a gold pan through friction welding. In this way they were protected from any new oxygen/water vapour inflow during annealing and consequently further oxidation was successfully prevented. In order to avoid bursting of the capsules owing to the raised inner pressure at higher temperatures the welding process took place at 300 hPa ambient pressure.

It has to be mentioned though, that the specimens had short contact with air during both the rotation at the sputter process and on their way to the sealing device. However, for temperatures lower than 900 K the stored energy measurements were neither influenced through these very thin oxide layers nor by the small portion of oxygen enclosed within the capsules [5, 9].

Sample preparation of the UHP Fe-150 ppm Nb alloy

Initially the samples of the Fe–Nb alloy were handled in the same way as just described. But since this material recrystallizes at essentially higher temperatures than the pure iron ([10] and further down) the gold capsules were replaced by platinum ones in order to avoid an eutectic reaction of the gold crucible and the platinum probe head of the calorimeter.

However, above 900 K the brief exposition of the samples to air during the preparation process showed up in the DSC measurements. So a new apparatus was constructed which could take on both the all-side sputtering and enclosing of the specimens in the same device without accompanying contact with air. The principal operation mode is as follows:

Figure 2a: First the iron sample lies loosely on a platinum lid which, for its part, is connected with a punch made of stainless steel. Above the sample an upside down crucible of platinum is fixed by a special mounting support while right in the middle of crucible and sample a moveable sheet metal (anode) can be introduced. By the ignition of a plasma between cathode (crucible, specimen and lid) and anode the top and the lateral surface of the iron cylinder are freed from oxides. The inside of the platinum pan can be cleaned as well.

Figure 2b: Next the anode is removed and punch and sample are shifted upwards together so that the specimen projects into the crucible. Now the entire sputter device is turned upside down and consequently the sample falls into the platinum pan.

Figure 2c: The punch is pulled away from the crucible and the anode is switched back again. Hence a newly initiated sputter process now cleans mainly the initial underside of the iron sample but also the platinum lid.

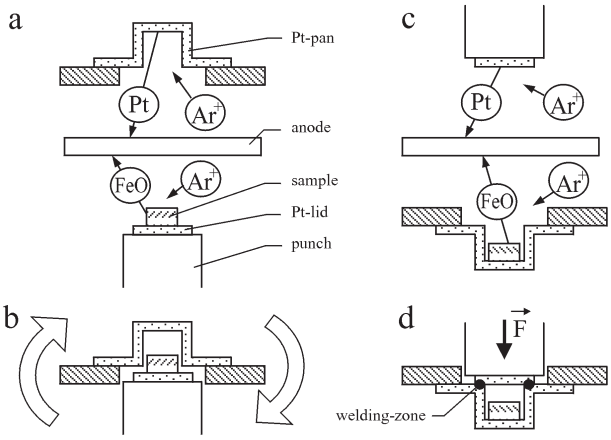

Fig. 2 Steps of the sputtering – sealing procedure

Figure 2d: Finally the specimen is encapsulated hermetically by friction welding the lid on the crucible.

Figures 2a–d: The total process takes place under vacuum or pure argon so that a contact between the freshly sputtered surface of the iron and air is completely impossible.

Since the platinum capsules tended to bulge at higher temperatures due to the increased inner pressure, the heat contact to the sensing probe of the calorimeter changed arbitrary. In order to avoid these samples of the Fe–Nb alloy were not enclosed under argon gas but vacuum (10^{-4} hPa).

Experimental procedure

Calorimetric measurements of the encapsulated samples were carried out under flowing argon in a power compensated DSC7 by Perkin Elmer (UHP Fe) and a Netzsch heat flux DSC 404C Pegasus (UHP Fe–Nb alloy), respectively, with heating rates between 10 and 40 K min^{-1}. The reference sample always consisted of annealed gold or platinum with a mass corresponding to the heat capacity of the iron sample and capsule at room temperature. In this way all observed heat flow signals can be traced back to reactions in the specimen and are not caused by the reference. As mentioned before, all measurements were repeated in order to obtain the baseline. Slight drifts in this 2nd run due to the repetition error of the calorimeters were then corrected in the heat flow difference according to Van der Plaats [11].

In order to examine whether the deformation of the capsules appeared in the heat flow signal already annealed iron samples were re-enclosed and measured again. Finally, the development of the microstructure was checked by terminating some DSC measurements at defined temperatures in the 1st run and preparing these samples for Vickers hardness tests and optical microscopy.

Results

The efficiency of the elaborate sample preparation procedure described in this paper is demonstrated by Fig. 3 where two consecutive measurements of an UHP Fe–Nb sample are plotted in the range close to the Curie temperature at 1042 K. Although the slope of the heat flow curve increases considerably due to the transition related change of the specific heat, the core of the recrystallization peak can already be suspected at ~980 K. Figure 3 does emphasize again that without a reliable baseline the stored energy release would not be noticed at all (Fig. 1).

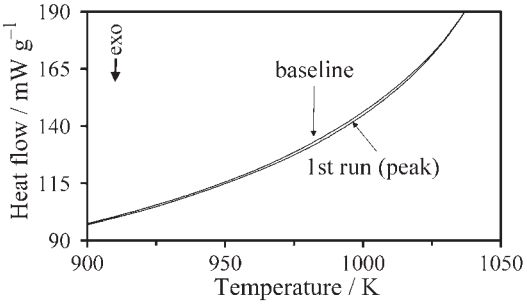

Fig. 3 Successive DSC measurements of UHP Fe–150 ppm Nb (cold rolled 80%) at β=20 K min^{-1} in a Netzsch DSC 404C Pegasus

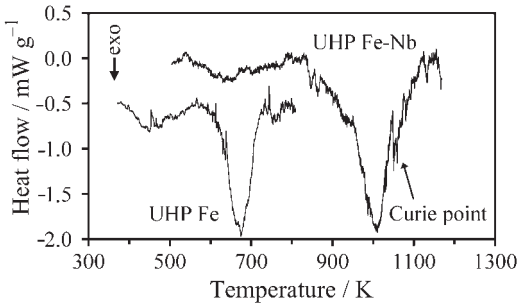

Fig. 4 Heat flow differences for both investigated materials (β=20 K min^{-1}). In order to avoid an overlap the measurement for the UHP iron was shifted vertically by –0.5 mW g^{-1} [10]

Exemplary heat flow differences for the energy release of pure iron and the Fe–Nb alloy are shown in Fig. 4 for a heating rate of 20 K min^{-1} [10]. Both curves consist of two exothermic peaks: one small, low-temperature reaction and a larger high-temperature one. The latter one for the niobium-doped iron is superimposed by a further peak indicated through an arrow in Fig. 4. This effect is caused by a small change of the Curie temperature of the original measurement (partially recrystallized state) and the baseline (fully recrystallized state). The same behaviour of the magnetic transition temperature is also observed in stored energy investigations of pure nickel, but is not further considered here.

The high-temperature reactions in Fig. 4 are clearly due to the recrystallization process as can be proved by optical micrographs and hardness investigations of partly annealed samples [5, 10]. On the other hand, since the overall deformation structure of the iron sample is retained up to the beginning of the main peaks and the hardness decreases only by a small amount up to this temperature range, it is suggested that recovery takes place during the low-temperature peaks in Fig. 4.

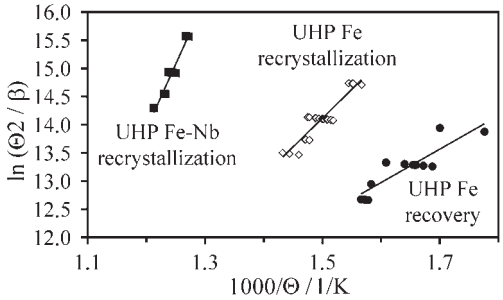

Fig. 5 Kissinger plot of Eq. (1) with heating rates between β=10 and 40 K min^{-1}. For better clarity some groups of experimental points were shifted horizontally by an arbitrary amount [9, 10]

Recovery and recrystallization are thermally activated processes. Hence, under the assumption that (independent of the heating rate β) the maximum transformation rate is correlated to the temperature Θ of the peak maximum, the activation enthalpies Q can be calculated using a simple Kissinger approach, where R is the universal gas constant [12] (Fig. 5):

$$\ln\left(\frac{\Theta^2}{\beta}\right) = \frac{Q}{R\Theta} + \text{const.} \qquad (1)$$

Analysis of the peak areas (Fig. 4) and of the fitted straight lines in Fig. 5 yields the mean stored energies and the activation enthalpies of recovery and recrystallization which are summarized in Table 1. However, the maximum of the comparatively shallow recovery peaks is rather ill defined. In fact, for the UHP Fe–Nb alloy no reliable value for the activation enthalpy of recovery can be given here.

Discussion

The stored energy release of 80% cold-rolled ultra high purity (UHP) iron during recovery and recrystallization amounts to a total about 20.5 J mol^{-1}. This is more than doubled by the addition of 150 ppm niobium (~46.7 J mol^{-1}) which indicates that the density of lattice defects after the same plastic deformation is larger in the Fe–Nb alloy than in the UHP iron.

This can be explained if one remembers that the essential elements of plastic deformation are the generation and movement of lattice defects, particularly of disloca-

tions. A certain fraction of them are annihilated at the surface of the metal or at other defect sinks (e.g. sub-grain boundaries) already during the deformation process. The niobium atoms of the alloy form a solid solution which means they are homogeneously incorporated into the iron lattice. Not having the same properties, i.e. the same size, these atoms will elastically distort the crystal lattice and act as obstacles for dislocation movement. Dislocations will be pinned which shows up in a higher yield stress or hardness, respectively. Further the pinned dislocations will lead to pile-ups of dislocations considerably increasing the dislocation density after deformation. Increasing the niobium concentration further on should initially lead to a further increase in hardness and stored energy. However, once the spacing of the piled-up dislocations and the distance of the niobium atoms in the iron lattice becomes similar no further increase can be expected.

Most probably a role of niobium carbide precipitates as pinning sites can be neglected in this connection since the carbon content in both materials investigated is very small (~1 ppm). In addition, first comparable calorimetric measurements of UHP iron with 360 ppm niobium (and therefore with the same amount of Nb–C precipitates as in the UHP Fe–150 ppm Nb alloy) indeed point to a further increase of the stored energy release, here about 50 J mol^{-1} are found for recrystallization on its own.

Table 1 The stored energies and activation enthalpies of recovery and recrystallization

	Recovery peak		Recrystallization peak	
	Stored energy/ J mol^{-1}	Activation enthalpy/kJ mol^{-1}	Stored energy/ J mol^{-1}	Activation enthalpy/kJ mol^{-1}
UHP Fe	3.1±0.3	49±7	17.4±0.8	85±8
UHP Fe–150 ppm Nb	10.6±1.4		36.1±2.0	206±22

Due to their diffusion-based character the activation enthalpies of recovery and recrystallization should correspond to those of the self-diffusion in iron (Q~260 kJ mol^{-1}) and of the diffusion of Nb in Fe (Q~259 kJ mol^{-1}), respectively [13]. This is in good agreement with the value presented in this paper for the activation enthalpy of the recrystallization process in the Fe–Nb alloy (Q~206 kJ mol^{-1}, Table 1).

For pure iron, however, activation enthalpies of Q~49 kJ mol^{-1} (recovery) and Q~85 kJ mol^{-1} (recrystallization), respectively, were determined in this investigation. These values are very small, even only half of the activation enthalpies given in the literature for the grain boundary self-diffusion in iron: Q~165 kJ mol^{-1} [13]. It has to be kept in mind though, that diffusion experiments of this kind were almost always carried out for less pure iron. And indeed, for iron without impurities segregated at grain boundaries or in solid solution an activation enthalpy of Q=91 kJ mol^{-1} is measured [14] which fits the value given in Table 1 for the recrystallization in UHP iron very well.

Conclusions

A new device is presented for sputtering and hermetically enclosing samples in noble metal capsules in the same apparatus without breaking the vacuum. The high efficiency of this sample treatment is demonstrated by preventing any oxidation reactions of iron specimens during annealing in a calorimeter without evacuating it. This makes it possible for the first time to investigate the stored energy release and the activation enthalpy of recovery and recrystallization in ultra high purity iron and an UHP Fe–Nb alloy. Of course, it is easily imaginable that this kind of sample preparation can be extremely useful also for other investigations.

* * *

The authors express their thanks to J. Driver and P. Jouffrey for the provision of the cold rolled iron. They are grateful to the Deutsche Forschungsgemeinschaft for financial support.

References

1 J. Schmidt, Thermochim. Acta, 151 (1989) 333.
2 F. Haessner, Proc. 1st Int. Conf. on Recrystallization in Metallic Materials (Recrystallization '90), T. Chandra (Ed.), The Minerals, Metals and Materials Society (TMS), Warrendale 1990, p. 511.
3 S. Sato, The Stored Energy of Cold Work, M. B. Bever, D. L. Holt and A. L. Titchener (Eds), Pergamon Press, Oxford 1973, p. 105.
4 T. Taoka, K. Suzuki, A. Yoshikawa and M. Okamato, Acta Metall., 13 (1965) 1311.
5 F. Scholz, J. H. Driver and E. Woldt, Scripta Mater., 40 (1999) 949.
6 A. F. Hollemann and E. Wiberg, Lehrbuch der anorganischen Chemie, Walter de Gruyter, Berlin 1971, p. 836.
7 G. W. H. Höhne, W. Hemminger and H.-J. Flammersheim, Differential Scanning Calorimetry, Springer Verlag, Berlin/Heidelberg 1996, p. 84.
8 J. LeCoze, R. Tardy, A. Kobylanski and M. Biscondi, Proc. 1st Int. Conf. on Ultra High Purity Base Metals (UHPM-94), The Japan Institute of Metals, Sendai 1995, p. 371.
9 F. Scholz, J. H. Driver and E. Woldt, Proc. Euromat´99: Microstructural Investigation and Analysis (Vol. 4), B. Jouffrey and J. Svejcar (Eds), Wiley-VCH, Weinheim 2000, p. 59.
10 F. Scholz and E. Woldt, Proc. 21st Risø Int. Symp. on Material Science, N. Hansen et al. (Eds), Risø National Laboratory, Roskilde, Denmark 2000, p. 563.
11 G. Van der Plaats, Thermochim. Acta, 72 (1984) 77.
12 H. E. Kissinger, Anal. Chem., 29 (1957) 1702.
13 I. Kaur, W. Gust and L. Kozma, Handbook of grain and interphase boundary diffusion data, Ziegler Press, Stuttgart 1989, p. 536.
14 H. Hänsel, L. Stratmann, H. Keller and H. J. Grabke, Acta Metall., 33 (1985) 659.